Journal of Alloys and Compounds 404–406 (2005) 537–540

Journal of ALLOYS AND COMPOUNDS

www.elsevier.com/locate/jallcom

Hydrogenation of nanocrystalline Zr–Fe–H powder

P. Roupcová[a,b,*], O. Schneeweiss[b], M. Zhu[c]

[a] *Institute of Materials Engineering, Brno University of Technology, Technická 2, 616 69 Brno, Czech Republic*
[b] *Institute of Physics of Materials, AS CR, Žižkova 22, 616 62 Brno, Czech Republic*
[c] *Department of Mechano-Electrical Engineering, South China University of Technology, Guangzhou, 510640 Guangdong, PR China*

Received 31 May 2004; received in revised form 4 March 2005; accepted 9 March 2005
Available online 20 July 2005

Abstract

Changes in the phase composition of nanocrystalline Zr–Fe powders prepared by spark synthesis were investigated in dependence of the heat treatment in vacuum and hydrogen atmosphere. Mössbauer spectroscopy, X-ray diffraction and magnetic measurements were applied for phase analysis. α-Fe, Fe embedded in ZrO_2, ZrO_2, and iron oxides were found in the as-prepared powder. After annealing in hydrogen, α-Fe and ZrO_2 dominate and minor Fe atoms embedded in ZrO_2 and Fe_2Zr were detected. Zr–Fe phases were transformed gradually into the α-Fe and ZrO_2 during the repeated annealing in vacuum and hydrogen. The ability of hydrogen absorption is decreasing with the annealing steps and is connected with the decrease of the Fe_2Zr phase content.

Keywords: Hydrogen storage materials; Spark synthesis; Mössbauer spectroscopy; X-ray diffraction

1. Introduction

Zr–Fe-based alloys are studied for magnetic properties and for the capability of hydrogen absorption in a broad temperature range. The nanoparticles of pure Zr and its intermetallic phases are sensitive to oxidation and they can be used as a getter protecting iron against oxidation during the heat treatment by preparation of magnetic nanocomposites in form of α-Fe nanoparticles embedded in a ZrO_2 matrix.

According to the equilibrium phase diagram the Fe–Zr system consists of the stable phases α-Fe, Fe_2Zr, $FeZr_2$ and metastable phases $FeZr_3$ and $Fe_3Zr(Fe_{23}Zr_6)$ [1,2]. For some Fe–Zr compositions the amorphous state can be fixed easily by rapid quenching from the melt. Amorphous Fe–Zr ribbons are interesting because of their magnetic properties and relatively high capacity of hydrogen absorption. Zr-based alloys and compounds are well known as materials for hydrogen storage. Hydrogenation of Zr–Fe alloys was described in [3]. It was shown that the ability of Zr-rich phases of absorbing of hydrogen led to a disproportionation and reproportionation of $FeZr_2$ and $FeZr_3$. Hydrogen absorbed at room temperature formed Zr_2FeH_5 hydride. The disproportionation of Zr_2Fe was unstable and it was very quickly followed by a reproportionation. This unusual behaviour was explained by the existence of an unstable ZrFe phase which is not described in any equilibrium Zr–Fe phase diagram. Nanocrystalline materials usually exhibit different physical properties in comparison with coarse polycrystals. The formation of metastable phases and pronounced hydrogen absorption can be expected [4–7].

Spark erosion is a possible alternative among the methods for preparing a new Zr–Fe phase simultaneously yielding nanocrystalline particles. This method was used for the preparation of amorphous, nanocrystalline or crystalline powder materials. The conditions of erosion are characterised by high temperature (above 10^4 K) and pressure (∼280 MPa) in a plasma channel, where a synthesis of the materials of electrodes with the surrounding occurs, and high cooling rate ($\sim 10^8$ K s^{-1}) [4,5]. It allows to overcome the solubility limits reached by classic alloying treatments and to synthesise new materials. Moreover, there are some possibilities to modify

* Corresponding author. Tel.: +420 532290447; fax: +420 541218657.
E-mail address: roupcova@ipm.cz (P. Roupcová).

0925-8388/$ – see front matter © 2005 Elsevier B.V. All rights reserved.
doi:10.1016/j.jallcom.2005.03.096

its composition by varying the parameters of sparks (e.g., voltage or time) and/or chemical composition, temperature and density (pressure) of the gaseous or liquid dielectrics.

In this paper we will describe some results obtained by the synthesis of Zr–Fe alloys with the aim of preparing nanocomposite materials consisting of iron and zirconium nanoparticles, focussing on the investigation of their phase composition in as-prepared and annealed state.

2. Experimental details

The nanopowder was prepared by spark synthesis of electrodes of pure Fe (99.99%) and Zr (99.9%) in a hydrogen atmosphere serving as dielectric [8,9]. The as-prepared powder was compacted (pressed) into pellets for heat treatments and magnetic measurements. The first annealing was carried out in pure hydrogen (better than 5N) atmosphere at 1030 K for 1 h. Subsequent annealing for hydrogen charging and discharging was carried out in hydrogen atmosphere and in a vacuum (10^{-2} Pa), respectively.

^{57}Fe Mössbauer spectra were collected by a standard transmission method at room temperature using a ^{57}Co/Rh source. The calibration of the spectra is referred relative to α-Fe at room temperature. The computer processing of the spectra was done by the CONFIT package [10] yielding by intensities I of the components (atomic fraction of Fe atoms), their hyperfine fields B_{hf}, isomer shifts δ and quadrupole splittings Δ.

Magnetic measurements were carried out using a vibrating sample magnetometer (VSM). The thermomagnetic curve was measured in the temperature range 293–1093 K with the sample in vacuum ($\sim 10^{-1}$ Pa).

X-ray powder diffraction (XRD) was performed using Co Kα radiation. Qualitative analysis was performed with the HighScore software and the JCPDS PDF-2 database. For a quantitative analysis of the XRD patterns we used Powder-Cell for Windows, Version 2.3 with structural models based on the ICSD database.

3. Results and discussion

The analysis of X-ray diffraction of the as-prepared powder material revealed iron, iron oxides (hematite, magnetite), tetragonal and monoclinic ZrO_2 phases. In its Mössbauer spectrum (Fig. 1) four sextets and four nonmagnetic components were recognised. The first sextet with B_{hf} =33.01 T, $\delta = 0.01$ mm/s, $\Delta = -0.01$ mm/s and $I = 0.09$ represents pure α-Fe phase, the second ($B_{hf} \sim 51.4$ T, $\delta = 0.38$ mm/s, $\Delta = -0.08$ mm/s, and $I = 0.07$), third and fourth sextets with ($B_{hf} \sim 48$ and 46 T, $\delta = 0.28$ and 0.66 mm/s, $\Delta = -0.08$ and 0.03 mm/s, and $I = 0.02$ and 0.01) can be ascribed to iron oxides (hematite and magnetite). The exact content and hyperfine parameters of iron oxides cannot be determined relatively small (nanocrystalline) size of the particles. Two doublets with $\delta = 0.30$ mm/s, $\Delta = 0.61$ mm/s, $I = 0.17$ and $\delta = 0.95$ mm/s, $\Delta = 0.28$ mm/s, $I = 0.49$ are explained as Fe^{3+} and Fe^{2+}. Those atoms were embedded in ZrO_2 in agreement with [11]. The iron atoms included in the ZrO_2 probably stabilise its tetragonal structure which is not stable at room temperature in a pure form. The doublet with $\delta = -0.36$ mm/s, $\Delta = 0.23$ mm/s, $I = 0.01$ represents $FeZr_3$. The last component represents fcc iron in ZrO_2 with $\delta = -0.08$ mm/s and $I = 0.31$. The high content of oxides is due to rapid oxidation of the as-prepared material during the opening of the preparation chamber. In some cases an increase of temperature of the powder was observed.

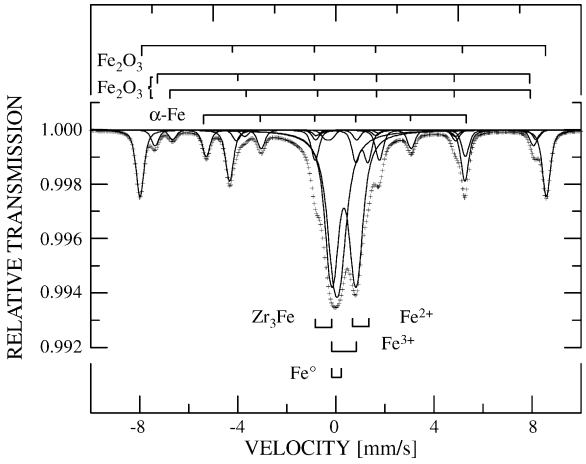

Fig. 1. Mössbauer spectrum of the as-prepared sample recorded at $T = 295$ K.

The change of the magnetic moment with temperature is shown in Fig. 2. Critical temperatures of the magnetic phase transition (Curie temperatures) of Fe_2Zr at 520 K and α-Fe at 1043 K can be identified. Fe_2Zr was recognised neither in X-ray diffractions nor in the Mössbauer spectrum. Two rea-

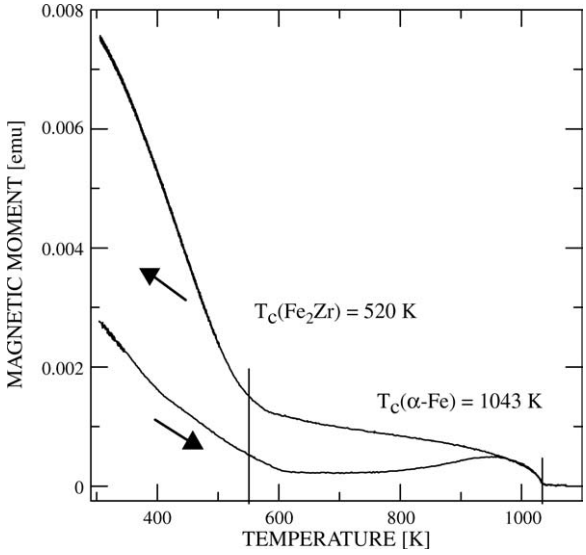

Fig. 2. Temperature dependence of the magnetic moment of the as-prepared sample.

Table 1
Phase composition derived from the Mössbauer spectra measured after the heat treatment steps

Step	Heat treatment	α-Fe	Fe_2Zr	$FeZr_3$	Fe^{2+} and Fe^{3+} in ZrO_2	fcc Fe	Fe_2O_3	Fe_3O_4
0	As-prepared	0.09	–	0.01	0.49	0.31	0.07	0.03
1	750 °C/1 h in H_2	0.78	0.06	–	0.12	0.04	–	–
2	787 °C/1 h in vacuum	0.72	0.11	–	0.12	0.04	–	–
3	785 °C/1 h in H_2	0.91	0.03	–	0.04	0.02	–	–
4	785 °C/1 h in vacuum	0.88	0.06	–	0.03	0.03	–	–
5	800 °C/10 h in H_2	0.9	0.04	–	0.04	0.02	–	–

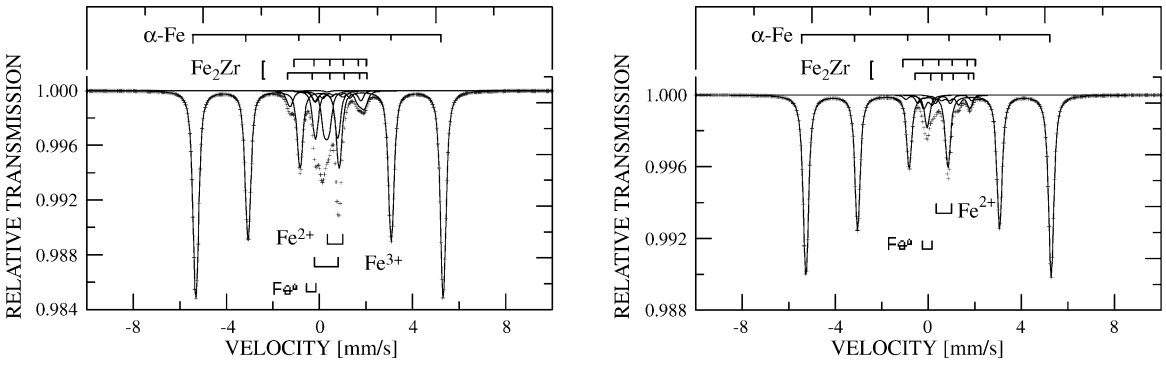

Fig. 3. Mössbauer spectrum of the sample recorded at $T = 295$ K after annealing in H_2 (left) and after annealing in vacuum (right).

sons for it can be expected: (i) the nanocrystalline character of the phase particles may cause that the size of coherent volumes are below the detection limit of X-ray diffraction, (ii) a strong overlapping with the other components and superparamagnetic behaviour disable its analysis in the Mössbauer spectrum. A slight increase in coercivity and remanence can be observed in the hysteresis loops measured before and after the thermomagnetic curve. This change can be ascribed to the increase in the mean size of the particles of the magnetic phases.

The phase analysis after the first heat treatment step – annealing in hydrogen at 750°C for 1 h – shows important changes in phase composition (see Table 1). The components of the iron oxides have diminished and the new sextets with $B_{hf} \sim 7$ and 5 T, $\delta = 0.5$ and 0.2 mm/s, $\Delta = -0.3$ and 0 mm/s, and $I = 0.04$ and 0.02 appeared. It can be ascribed to Fe_2Zr according to the phase transition (Curie) temperature found in temperature dependence of the magnetic moment. However its hyperfine field significantly differs from the stoichiometric (bulk) Fe_2Zr phase probably due to small particle volumes and broad particle size distribution [12].

The next two steps of annealing in vacuum followed by annealing in hydrogen caused fine changes in the phase composition only. Examples of the Mössbauer spectra are shown in Fig. 3. They are characterised by a decreasing content of α-Fe after annealing in vacuum in favour of the other magnetic components. The contents of the other phases have decreased in all steps of the heat treatment. It is probably due to a segregation of Fe atoms and the formation of larger α-Fe particles. This explanation can be also supported by X-ray diffraction after the steps of heat treatment. ZrO_2 has transformed in to the monoclinic stable form (baddellyite). Other phases were below the detection limit of the experiment.

The above results based on Mössbauer phase analysis do not confirm the hydrogen-induced disproportionation Zr_2Fe and Fe_2Zr phases to Zr_3Fe described in [3]. We have observed that the magnetic phase Fe_2Zr transformed in consequence of hydrogenation to pure α-Fe and nonmagnetic phases (Fe, Fe^{3+} and Fe^{2+} in ZrO_2).

4. Conclusions

Nanocrystalline Zr–Fe powder prepared by spark synthesis of the pure Zr and Fe electrodes in hydrogen consists of a mixture of amorphous and nanocrystalline components that are able to absorb hydrogen. The phases α-Fe, Fe embedded in ZrO_2, ZrO_2, Fe_2O_3, and Fe_3O_4 were found in the as-prepared state. After the first annealing in hydrogen, α-Fe, ZrO_2, Fe atoms embedded in ZrO_2, and Fe_2Zr were detected. Fe–Zr phases transformed into α-Fe and ZrO_2 during the subsequent annealing in vacuum and hydrogen. The ability of hydrogen absorption was decrease with the annealing steps. The loss of the ability to absorb hydrogen is connected with the decrease of the Fe_2Zr phase content.

Acknowledgements

This work was supported by the Czech Ministry of Education, Youth and Sports (FRVS 1528, ME636) and the Academy of Sciences of the Czech Republic (K10101040).

References

[1] H. Okamoto, J. Phase Equilibr. 14 (5) (1993).
[2] F. Aubertin, U. Gonser, S.J. Cambell, H.G. Wagner, Z. Metall. 76 (1985) 237–244.
[3] M. Hara, R. Hayakawa, Y. Kaneko, K. Watanabe, J. Alloys Compd. 352 (2003) 218–225.
[4] A. Zaluska, L. Zaluski, J.O. Strom-Olsen, Appl. Phys. A 72 (2001) 157–165.
[5] L. Chen, F. Wu, M. Tong, B.R. Long, Z.Q. Shang, H. Liu, W.S. Sun, K. Yang, L.B. Wang, Y.Y. Li, J. Alloys Compd. 293 (1999) 508–520.
[6] U. Koster, D. Zander, Triwikantoro, A. Rudiger, L. Jastrow, Scripta Mater. 44 (2001) 1649–1654.
[7] T. Klassen, R. Bohn, G. Fanta, W. Oelerich, N. Eigen, F. Gartner, E. Aust, R. Bormann, H. Kreye, Z. Metall. 94 (2003) 610–614.
[8] J.L. Walter, Powder Metall. 31 (1988) 267.
[9] A.E. Berkowitz, J.L. Walter, Mater. Sci. Eng. 55 (1982) 275.
[10] T. Žák, in: M. Miglierini, D. Petridis (Eds.), Mössbauer Spectroscopy in Materials Science, Kluwer Academic Publishers, Dordrecht, 1999, p. 385.
[11] E. Kuzmann, M.L. Varsanui, K. Nomura, Y. Ujihira, T. Masumoto, G. Principi, C. Tosello, K. Havancsak, A. Vértes, Electrochem. Commun. 2 (2000) 130–134.
[12] A. Govaert, C. Dauwe, P. Plinke, E. de Grave, J. de Sitter, J. Phys. 37 (1976) 6–825.